Multicomponent van der Waals equation of state: Applications in nuclear and hadronic physics

Volodymyr Vovchenko,[1,2,3] Anton Motornenko,[3,4,2] Paolo Alba,[2] Mark I. Gorenstein,[5,2]
Leonid M. Satarov,[2,6] and Horst Stoecker[1,2,7]

[1]*Institut für Theoretische Physik, Goethe Universität Frankfurt, D-60438 Frankfurt am Main, Germany*
[2]*Frankfurt Institute for Advanced Studies, Giersch Science Center, D-60438 Frankfurt am Main, Germany*
[3]*Department of Physics, Taras Shevchenko National University of Kiev, 03022 Kiev, Ukraine*
[4]*Department of Physics, University of Oslo, 0313 Oslo, Norway*
[5]*Bogolyubov Institute for Theoretical Physics, 03680 Kiev, Ukraine*
[6]*National Research Center, "Kurchatov Institute," 123182 Moscow, Russia*
[7]*GSI Helmholtzzentrum für Schwerionenforschung GmbH, D-64291 Darmstadt, Germany*

A generalization of the quantum van der Waals equation of state for a multicomponent system in the grand-canonical ensemble is proposed. The model includes quantum statistical effects and allows us to specify the parameters characterizing repulsive and attractive forces for each pair of particle species. The model is applied to the description of asymmetric nuclear matter and also for mixtures of interacting nucleons and nuclei. Applications of the model to the equation of state of an interacting hadron resonance gas are discussed.

I. INTRODUCTION

The equation of state of hot, dense strongly interacting matter has been the focus of experimental and theoretical investigations of high-energy heavy-ion collisions. Thermal models were constructed [1–10] to describe yields of secondary hadrons and nuclear fragments from such collisions. These models assume that the emitted particles stem from a statistically equilibrated system. The temperature T and baryon chemical potential μ_B of the emitting source are obtained by fitting the observed yields of stable hadrons. In most cases, the ideal hadron resonance gas (I-HRG) model has been used. A surprisingly good description of many experimental hadron yield data from heavy-ion collisions have been achieved within this simple approach for a broad range of collision energies (see, e.g., Ref. [11] and references therein). The T-μ_B values fitted in the I-HRG model show, however, that hadron densities are rather large at the chemical freeze-out stage of the reaction. Therefore, one can expect residual interactions, leading to significant deviations from the ideal gas picture.

Phenomenological models of the phase structure of nuclear matter also show [12,13] that a realistic phase diagram cannot be obtained without an explicit account of the hadronic interactions. Extensions of the ideal gas picture have been discussed mostly within the excluded volume HRG model, in which the effects of various hadron's repulsions at short distances have been introduced (see, e.g., Ref. [14] and references therein).

The presence of both repulsive and attractive interactions between nucleons is evident from the existence of stable nuclei. These interactions should also be taken into account to describe the simple binding properties of nuclear matter and the multifragmentation observed at intermediate energy nucleus-nucleus collisions. Recently, nuclear matter has been modeled as van der Waals (vdW) fluid of interacting nucleons

[15]. The vdW parameters a and b describe, respectively, attractive and repulsive vdW interactions. a and b are fixed by fitting the nucleon number density and binding energy per nucleon at $T = 0$. Attractive and repulsive interactions between nucleons were also discussed within the mean-field theory (see Ref. [16] and references therein). vdW interactions between baryons, and between antibaryons, respectively, were considered within a quantum vdW-HRG model in Ref. [17].

This paper presents general formulation of the quantum van der Waals (QvdW) model, with different repulsive and attractive interactions in the multicomponent system of different particle species. Classical multicomponent vdW description is done for the pressure as a function of the temperature T and the particle number densities n_i $(i = 1, \ldots, h)$ in the canonical ensemble (CE): $p = p(T, n_1, \ldots, n_h)$. To proceed further, the free energy F is reconstructed. F is the thermodynamical potential in the CE. At this stage, we introduce quantum statistics. Note that a quantum vdW model was previously formulated for a single constituent type only [17].

Next, the model formulation is transformed to the grand-canonical ensemble (GCE). Reference [18] shows that this transformation is important for several reasons. Note that the chemical potentials—and *not* the particle densities—and the temperature are the natural variables of the pressure function $p = p(T, \mu_1, \ldots, \mu_h)$.

Section II presents the multicomponent vdW model in the CE and introduces the effects of quantum statistics. Section III presents the GCE formulation. Section IV discusses the applications of the developed formalism. Many applications of the multicomponent QvdW equation are in sight: A first example is a model of nuclear matter that includes a mixture of interacting protons, neutrons, and nuclei. A second example is the multicomponent QvdW HRG. Section V summarizes the paper.

II. CANONICAL ENSEMBLE FORMULATION

The classical multicomponent system with vdW interactions is defined within the CE in terms of the following pressure function:

$$p(T, n_1, \ldots, n_h) = \sum_i \frac{T\, n_i}{1 - \sum_j \tilde{b}_{ji}\, n_j} - \sum_{i,j} a_{ij}\, n_i\, n_j, \quad (1)$$

where n_i is the particle density for the ith species ($i = 1, \ldots, h$) and T is the system's temperature. The parameters a_{ij} and $\tilde{b}_{ji}$ in Eq. (1) yield the attractive and repulsive vdW interactions, respectively. The repulsive vdW interactions amount to the excluded volume (EV) correction. For particles with the classical hard-core interaction one has [19]

$$\tilde{b}_{ij} = 2 b_{ii} b_{ij} / (b_{ii} + b_{jj}), \quad (2)$$

where $b_{ij} = 2\pi (r_i + r_j)^3 / 3$ is the symmetric matrix of the second-order virial coefficients, r_i being the hard-core radius for the ith particle species. In a more general case, $\tilde{b}_{ij}$ should be regarded as phenomenological parameters, characterizing the strength of the repulsive interactions between different pairs of particle species.

The free energy $F(T, V, \{N_i\})$ in the CE reads [14]:

$$F(T, V, \{N_i\}) = \sum_i F_i^{\mathrm{id}}\left(T, V - \sum_j \tilde{b}_{ji} N_j, N_i\right)$$
$$- \sum_{i,j} a_{ij} \frac{N_i N_j}{V}. \quad (3)$$

The function $F_i^{\mathrm{id}}(T, V, N_i)$ is the free energy of the classical (Boltzmann) ideal gas for species i ($\hbar = c = 1$):

$$F_i^{\mathrm{id}}(T, V, N_i) = -N_i T \left[1 + \ln \frac{g_i V m_i^2 T K_2(m_i/T)}{2\pi^2 N_i} \right]. \quad (4)$$

Here m_i is the mass of particle species i, g_i is the particle degeneracy factor (i.e., the number of internal states), and K_2 is the modified Bessel function. Note that the free energy F is a genuine thermodynamic potential in the CE. F gives the complete information about the statistical system considered. The partial derivative of F (3) over the system volume, $p = -(\partial F/\partial V)_{T,\{N_i\}}$, yields the vdW pressure (1). Note that free energy (3) depends on the parameters $\{m_i\}$ and $\{g_i\}$, but these parameters are absent in the vdW pressure (1) in the CE.

Expressions (1) and (3) do not include the effects of quantum statistics. The classical free energies of an ideal gas F_i^{id} in Eq. (4) are replaced by the ideal *quantum* gas expressions (Fermi-Dirac or Bose-Einstein) in order to include these effects. This procedure satisfies the following consistency requirements: It leads to a mixture of the ideal quantum gases if all $\tilde{b}_{ij} = 0$ and $a_{ij} = 0$. It gives the correct limiting classical expressions (1) in the regions of the thermodynamic parameters where quantum statistics can be neglected. Finally, the entropy obtained for the QvdW expressions is positive definite, $S \geqslant 0$, and it respects Nernst's theorem, $S \to 0$ at $T \to 0$. Quantum statistics of the one-component vdW fluid has been considered in Refs. [15,20,21].

Using this quantum statistical free energy, one can calculate all other thermodynamic functions in the CE: pressure p, total

entropy S, and energy E of the system, as well as the ith chemical potential μ_i:

$$p(T, \{n_k\}) \equiv -\left(\frac{\partial F}{\partial V}\right)_{T,\{N_j\}} = \sum_i p_i^{\mathrm{id}}\left(T, \frac{n_i}{f_i}\right)$$
$$- \sum_{i,j} a_{ij}\, n_i\, n_j, \quad (5)$$

$$S(T, V, \{N_k\}) \equiv -\left(\frac{\partial F}{\partial T}\right)_{V,\{N_j\}} = V \sum_i f_i\, s_i^{\mathrm{id}}\left(T, \frac{n_i}{f_i}\right), \quad (6)$$

$$E(T, V, \{N_k\}) \equiv F + TS = V \sum_i f_i\, \varepsilon_i^{\mathrm{id}}\left(T, \frac{n_i}{f_i}\right)$$
$$- V \sum_{i,j} a_{ij}\, n_i\, n_j, \quad (7)$$

$$\mu_i(T, \{n_k\}) \equiv \left(\frac{\partial F}{\partial N_i}\right)_{T,V,\{N_{j\neq i}\}} = \mu_i^{\mathrm{id}}\left(T, \frac{n_i}{f_i}\right)$$
$$+ \sum_j \tilde{b}_{ij}\, p_j^{\mathrm{id}}\left(T, \frac{n_j}{f_j}\right) - \sum_j (a_{ij} + a_{ji})\, n_j. \quad (8)$$

Here $f_i \equiv 1 - \sum_j \tilde{b}_{ji} n_j$ quantifies the fraction of the total volume which is available for particles at the given densities values and p_i^{id}, s_i^{id}, $\varepsilon_i^{\mathrm{id}}$, and μ_i^{id} are the ideal quantum gas expressions for the CE pressure, entropy density, energy density, and chemical potential for ith particle species, respectively, as functions of temperature and particle number density.

III. GRAND-CANONICAL ENSEMBLE FORMULATION

In the GCE, the thermodynamic variables are the temperature T and the set of chemical potentials $\{\mu_k\}$. The particle densities $\{n_k\}$, on the other hand, are not the independent variables anymore in the GCE. Instead, they become functions of the T and $\{\mu_k\}$. The pressure function $p(T, \{\mu_k\})$ defines all thermodynamic properties of the system in this ensemble.

Both the CE and the GCE are equivalent for describing the thermodynamic properties in the thermodynamic limit, $V \to \infty$. This fact can be used to transform the multicomponent QvdW model from the CE to the GCE: It is sufficient only to derive the function $p(T, \{\mu_k\})$ from Eqs. (5)–(8).

First, let us introduce the notations

$$p_i^* \equiv p_i^{\mathrm{id}}\left(T, \frac{n_i}{f_i}\right), \quad n_i^* \equiv n_i^{\mathrm{id}}\left(T, \frac{n_i}{f_i}\right), \quad s_i^* \equiv s_i^{\mathrm{id}}\left(T, \frac{n_i}{f_i}\right), \quad (9)$$

and

$$\mu_i^* \equiv \mu_i^{\mathrm{id}}\left(T, \frac{n_i}{f_i}\right). \quad (10)$$

Here all the ideal gas functions correspond to the CE. Equation (10) can be inverted to yield:

$$\frac{n_i}{f_i} = n_i^{\mathrm{id}}(T, \mu_i^*), \quad i = 1, \ldots, h, \quad (11)$$

where $n_i^{\mathrm{id}}(T,\mu_i^*)$ is now the GCE ideal gas density at temperature T and chemical potential μ_i^*. Using (11) one can rewrite Eqs. (9) as

$$p_i^* = p_i^{\mathrm{id}}(T,\mu_i^*), \quad n_i^* = n_i^{\mathrm{id}}(T,\mu_i^*), \quad s_i^* = s_i^{\mathrm{id}}(T,\mu_i^*),$$
(12)

where all the ideal gas functions in (12) correspond to the GCE. Therefore, the GCE pressure reads

$$p(T,\{\mu_i\}) = \sum_i p_i^* - \sum_{i,j} a_{ij}\, n_i\, n_j.$$
(13)

Equations (11) can be rewritten as the system of linear equations for particle densities n_i:

$$\sum_j (\delta_{ij} + \tilde{b}_{ji}\, n_i^*)\, n_j = n_i^*, \quad i = 1,\dots,h.$$
(14)

If the μ_i^*, at given T and μ_i, are known, then all other quantities, in particular, the system pressure (13), can be calculated as well. Indeed, the calculations of p_i^* and n_i^* are straightforward, while n_i can be recovered by solving the system of linear equations (14). Finally, the pressure is obtained by substituting p_i^* and n_i into (13). All other thermodynamic functions in the GCE are obtained from the pressure function $p(T,\{\mu_i\})$ using standard thermodynamic relations.

Using the above notations, one can rewrite (8) as

$$\mu_i^* + \sum_j \tilde{b}_{ij}\, p_j^* - \sum_j (a_{ij} + a_{ji})\, n_j = \mu_i, \quad i = 1,\dots,h.$$
(15)

Solution to this system of transcendental equations determines $\{\mu_i^*\}$ at given T and $\{\mu_i\}$. In general, this solution should be obtained numerically. Once the effective chemical potentials $\{\mu_i^*\}$ are specified, all other quantities can be calculated directly. If multiple solutions of equations (15) are found, then the solution with the largest pressure is the physical result according to the Gibbs criterion.

The GCE entropy and energy densities are given as

$$s(T,\{\mu_i\}) \equiv \left(\frac{\partial p}{\partial T}\right)_{\{\mu_j\}} = \sum_i f_i\, s_i^*,$$
(16)

$$\varepsilon(T,\{\mu_i\}) \equiv \left(\frac{\partial p}{\partial T}\right)_{\{\mu_j\}} + \sum_i \mu_i \left(\frac{\partial p}{\partial \mu_i}\right)_{T,\{\mu_{j\neq i}\}} - p$$

$$= \sum_i f_i\, \varepsilon_i^* - \sum_{i,j} a_{ij}\, n_i\, n_j.$$
(17)

Here $\varepsilon_i^* = \varepsilon_i^{\mathrm{id}}(T,\mu_i^*)$.

IV. APPLICATIONS

The new multicomponent QvdW formalism presented here is applied to the following three examples.

A. Asymmetric nuclear matter as a QvdW mixture of protons and neutrons

Nuclear matter is a hypothetical infinite system of interacting protons and neutrons which is approximately realized in nature in the interior of massive nuclei and in neutron stars. The thermodynamic equilibrium in such a system can be specified by the temperature, T, and proton and neutron densities, n_p and n_n. Nucleon-nucleon interactions exhibit repulsion at short distances and attraction at intermediate ones. Hence, it makes sense to model such a system by a QvdW equation. The multicomponent QvdW equation for protons and neutrons then reads

$$p(T,n_p,n_n) = p_p^{\mathrm{id}}\left(T, \frac{n_p}{f_p}\right) + p_n^{\mathrm{id}}\left(T, \frac{n_n}{f_n}\right) - a_{pp}\, n_p^2$$

$$- a_{pn}\, n_p\, n_n - a_{np}\, n_n\, n_p - a_{nn}\, n_n^2, \quad (18)$$

where $f_p = 1 - \tilde{b}_{pp}\, n_p - \tilde{b}_{np}\, n_n$ and $f_n = 1 - \tilde{b}_{pn}\, n_p - \tilde{b}_{nn}\, n_n$. Isospin symmetry yields $m_p = m_n \simeq 938\,\mathrm{MeV}/c^2$, $\tilde{b}_{pp} = \tilde{b}_{nn}$, $\tilde{b}_{pn} = \tilde{b}_{np}$, $a_{pp} = a_{nn}$, and $a_{pn} = a_{np}$. This model has only four interactions parameters: $\tilde{b}_{pp}$, $\tilde{b}_{pn}$, a_{pp}, and a_{pn}. These correspond to isospin-dependent nucleon-nucleon interactions.

The asymmetry of the nuclear matter is characterized by the proton fraction $y = n_p/(n_p + n_n)$, which takes values between 0 and 1, and the total nucleon density $n_N = n_p + n_n$. The value $y = 1/2$ corresponds to the symmetric nuclear matter, i.e., the numbers of protons and neutrons in the system are equal. In this case, Eq. (18) reduces to a single-component QvdW equation for nucleons,

$$p(T,n_N,y = 1/2) = p_N^{\mathrm{id}}\left(T, \frac{n_N}{1 - b_{NN}\, n_N}\right) - a_{NN}\, n_N^2. \quad (19)$$

Here the nucleon ideal gas pressure p_N^{id} contains the spin-isospin nucleon degeneracy factor $g_N = 4$, and

$$a_{NN} = \frac{a_{pp} + a_{pn}}{2} \quad \text{and} \quad \tilde{b}_{NN} = \frac{\tilde{b}_{pp} + \tilde{b}_{pn}}{2}. \quad (20)$$

Equation (19) coincides with the model used in Ref. [15]. The parameters a_{NN} and $\tilde{b}_{NN}$ are fixed by reproducing the binding energy $\varepsilon/n_N - m_N = -16\,\mathrm{MeV}$ at saturation density $n_0 = 0.16\,\mathrm{fm}^{-3}$. The following parameter values are obtained: $a_{NN} \simeq 329\,\mathrm{MeV\,fm}^3$ and $\tilde{b}_{NN} \simeq 3.42\,\mathrm{fm}^3$.

In the present work these a_{NN} and $\tilde{b}_{NN}$ values are used, while the a_{pn}/a_{pp} and $\tilde{b}_{pn}/\tilde{b}_{pp}$ ratios are taken as free parameters. Variations in these ratios correspond to different scenarios for the isospin dependence of the nucleon-nucleon potential.

Cold nuclear matter with $T = 0$ is considered. The nuclear symmetry energy $S(n)$ is sensitive to the isospin part of the nucleon-nucleon interactions. It characterizes the dependence of the energy per nucleon $E/A \equiv \varepsilon/n_N - m_N$ on the proton fraction y. The widely used parabolic approximation represents E/A as

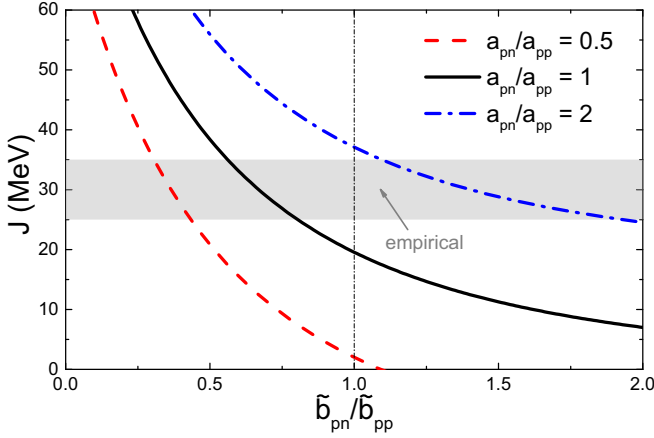$$E/A\,(n,y) \approx E/A\,(n,y = 1/2) + 4\,S(n)\,(y - 1/2)^2. \quad (21)$$

FIG. 1. Dependence of the symmetry energy J on the ratio $\tilde{b}_{pn}/\tilde{b}_{pp}$ of the repulsive vdW parameters for three different values of the ratio a_{pn}/a_{pp} of the attractive vdW parameters. Variations in these ratios probe the isospin dependence of the nucleon-nucleon potential.

The symmetry energy at saturation density, defined as

$$J \equiv S(n_0) = \frac{1}{8} \left.\frac{\partial^2 (E/A)}{\partial y^2}\right|_{n_N = n_0,\, y=1/2}, \quad (22)$$

corresponds roughly to the difference of the energy per nucleon at $n_N = n_0 \simeq 0.16 \text{ fm}^{-3}$ for pure neutron matter ($y = 0$) and symmetric nuclear matter ($y = 1/2$).

The dependence of J on different values of the a_{pn}/a_{pp} and $\tilde{b}_{pn}/\tilde{b}_{pp}$ ratios is shown in Fig. 1. The empirical range $J \simeq 25-35$ MeV [22] is depicted by the shaded area. In the fully symmetric scenario, i.e., for $a_{pp} = a_{pn} = a_{NN}$ and $\tilde{b}_{pp} = \tilde{b}_{pn} = \tilde{b}_{NN}$, the value of the symmetry energy $J \simeq 18$ MeV underestimates significantly the empirical estimates. In this case the total symmetry energy value is attributed solely to the decrease of the spin-isospin degeneracy factor, from 4 in symmetric nuclear matter to 2 in pure neutron matter. This mechanism is not sufficient to describe the empirical data. On the other hand, either an increase in a_{pn} or a reduction in $\tilde{b}_{pn}$ improves the agreement with the data.

More stringent restrictions on the values of parameters a_{pn} and $\tilde{b}_{pn}$ can be obtained by analyzing additional observables. These may include the density dependence of the symmetry energy or the higher-order terms of expansion (21) of the E/A in terms of the proton fraction y.

B. Mixture of interacting nucleons and α particles

Light nuclei ought to be included in models of nuclear matter. A simple example is a mixture of nucleons and α particles in symmetric nuclear matter, i.e., $n_p = n_n$. The baryon number $B = N_N + 4N_\alpha$ is conserved in this system, but the numbers of nucleons, N_N, and α's, N_α, are not conserved separately. The chemically equilibrated $N-\alpha$ mixture has one independent baryonic chemical potential μ which regulates the baryonic density $n \equiv n_N + 4n_\alpha$. The chemical potentials of nucleons and alphas are $\mu_N = \mu$ and $\mu_\alpha = 4\mu$, and the α binding energy is contained in the α mass. The pressure of the

system is (1)

$$p = p_N^* + p_\alpha^* - a_{NN}\,n_N^2 - a_{N\alpha}\,n_N n_\alpha - a_{\alpha N} n_\alpha n_N - a_{\alpha\alpha}\,n_\alpha^2. \quad (23)$$

Here

$$p_N^* \equiv p_N^{\text{id}}(T,\mu_N^*) = \frac{g_N}{6\pi^2} \int_0^\infty \frac{dk\,k^4}{\sqrt{m_N^2 + k^2}}$$

$$\times \left[\exp\left(\frac{\sqrt{m_N^2 + k^2} - \mu_N^*}{T} \right) + 1 \right]^{-1}, \quad (24)$$

$$p_\alpha^* \equiv p_\alpha^{\text{id}}(T,\mu_\alpha^*) = \frac{g_\alpha}{6\pi^2} \int_0^\infty \frac{dk\,k^4}{\sqrt{m_\alpha^2 + k^2}}$$

$$\times \left[\exp\left(\frac{\sqrt{m_\alpha^2 + k^2} - \mu_\alpha^*}{T} \right) - 1 \right]^{-1}, \quad (25)$$

and $m_N \simeq 938$ MeV, $g_N = 4$, $m_\alpha \simeq 4m_N - 28.3$ MeV, and $g_\alpha = 1$.

The system of linear equations (14) can be explicitly solved to yield

$$n_N = \frac{n_N^*[1 + (\tilde{b}_{\alpha\alpha} - \tilde{b}_{\alpha N})\,n_\alpha^*]}{1 + \tilde{b}_{NN}\,n_N^* + \tilde{b}_{\alpha\alpha}\,n_\alpha^* + (\tilde{b}_{NN}\,\tilde{b}_{\alpha\alpha} - \tilde{b}_{N\alpha}\,\tilde{b}_{\alpha N})\,n_N^*\,n_\alpha^*}, \quad (26)$$

$$n_\alpha = \frac{n_\alpha^*[1 + (\tilde{b}_{NN} - \tilde{b}_{N\alpha})\,n_N^*]}{1 + \tilde{b}_{NN}\,n_N^* + \tilde{b}_{\alpha\alpha}\,n_\alpha^* + (\tilde{b}_{NN}\,\tilde{b}_{\alpha\alpha} - \tilde{b}_{N\alpha}\,\tilde{b}_{\alpha N})\,n_N^*\,n_\alpha^*}. \quad (27)$$

Here

$$n_N^* \equiv n_N^{\text{id}}(T,\mu_N^*) = \frac{g_N}{2\pi^2} \int_0^\infty dk\,k^2$$

$$\times \left[\exp\left(\frac{\sqrt{m_N^2 + k^2} - \mu_N^*}{T} \right) + 1 \right]^{-1}, \quad (28)$$

$$n_\alpha^* \equiv n_\alpha^{\text{id}}(T,\mu_\alpha^*) = \frac{g_\alpha}{2\pi^2} \int_0^\infty dk\,k^2$$

$$\times \left[\exp\left(\frac{\sqrt{m_\alpha^2 + k^2} - \mu_\alpha^*}{T} \right) - 1 \right]^{-1}. \quad (29)$$

The quantities $\tilde{b}_{ij}$ are given by Eq (2) in terms of hard-core radii r_N and r_α.

The system of Eqs. (15) should be solved with respect to μ_N^* and μ_α^* at given T and μ. It reads

$$\mu_N^* = \mu - \tilde{b}_{NN}\,p_N^* - \tilde{b}_{N\alpha}\,p_\alpha^* + 2\,a_{NN}\,n_N + (a_{N\alpha} + a_{\alpha N})n_\alpha,$$

$$\mu_\alpha^* = 4\mu - \tilde{b}_{\alpha N}\,p_N^* - \tilde{b}_{\alpha\alpha}\,p_\alpha^* + 2\,a_{\alpha\alpha}\,n_\alpha + (a_{\alpha N} + a_{N\alpha})n_N. \quad (30)$$

The system of equations for μ_N^* and μ_α^* can be solved numerically. The system pressure (23) and all other thermodynamical functions can be calculated once the effective chemical potentials μ_N^* and μ_α^* are found. The solution with the largest pressure is taken if multiple solutions appear at a given

TABLE I. Thermodynamical properties of the mixture of interacting nucleons and α particles at the critical point. The results are compared to the case of pure nucleon matter [15].

	T_c (MeV)	μ_c (MeV)	n_c (fm^{-3})	p_c (MeV fm^{-3})	X_α
$N + \alpha$ mix.	19.90	907.56	0.0733	0.562	0.013
Pure N	19.68	907.67	0.0723	0.525	0

μ-T pair, in accordance with the Gibbs criterion: This means that only the states corresponding to global thermodynamic equilibrium are considered in the present work.

The following QvdW parameters reproduce the known properties of the nuclear ground state [15]:

$$a_{NN} = 329 \text{ MeV fm}^3 \quad \text{and} \quad \widetilde{b}_{NN} = 3.42 \text{ fm}^3. \quad (31)$$

For simplicity, attractive vdW interactions involving α particles are neglected, i.e.,

$$a_{\alpha\alpha} = a_{\alpha N} = a_{N\alpha} = 0, \quad (32)$$

but repulsive EV interactions between α-α pairs and between α-N pairs are included, an effective hard-core radius of $r_\alpha = 1$ fm is assumed. This entails

$$\widetilde{b}_{\alpha\alpha} = \frac{16\pi r_\alpha^3}{3} \simeq 16.76 \text{ fm}^3. \quad (33)$$

The EV cross terms are calculated according to (2). This gives

$$\widetilde{b}_{\alpha N} \simeq 13.95 \text{ fm}^3 \quad \text{and} \quad \widetilde{b}_{N\alpha} \simeq 2.85 \text{ fm}^3. \quad (34)$$

The phase diagram for the $N-\alpha$ mixture is shown in Fig. 2 in the (μ, T) plane. The parameters of the critical point (CP) are presented in Table I. They are compared to the corresponding results for pure nucleon matter. The addition of α particles to the model does lead to small changes in the phase diagram of this toy model of nuclear matter. The phase diagram is very similar to the pure nucleon system [15]. A slight change in the location of the CP of nuclear matter yields a shift in critical temperature T_c from 19.68 MeV to 19.90 MeV. The critical baryon density n_c increases from 0.0723 fm^{-3} to 0.0733 fm^{-3} (see Table I). The "mass fraction" of α particles, $X_\alpha = 4n_\alpha/(n_N + 4n_\alpha)$, is approximately, 1.3% at the CP.
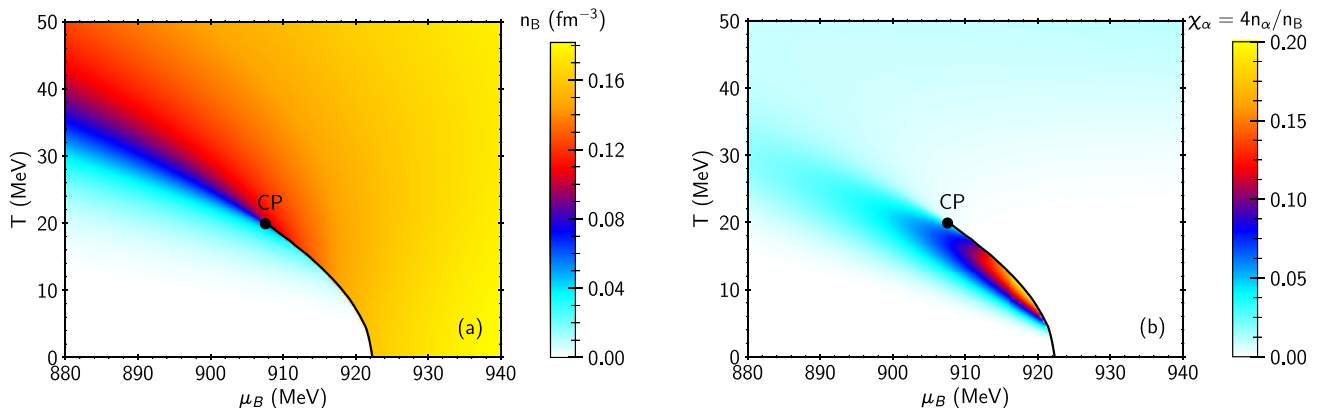

FIG. 3. Dependence of the α mass fraction X_α on the baryon chemical potential μ for three different isotherms. The dashed red line corresponds to $T = T_c/2 \simeq 10$ MeV, half the critical temperature. The solid black line corresponds to the critical isotherm $T = T_c \simeq 19.89$ MeV. The dash-dotted blue line corresponds to $T = 3T_c/2 \simeq 30$ MeV, above the critical temperature.

The behavior of the α mass fraction, X_α, is shown in Fig. 2(b) in the (μ, T) plane. X_α jumps from approximately 0.2 to a negligibly small value across the phase transition line at $T = T_c/2$. A noticeable fraction is present just below the phase transition line. This jump is caused by the repulsive EV interactions between nucleons and α particles, which suppress the bigger α particles in dense nuclear matter.

The dependence of X_α on the baryochemical potential μ is shown in Fig. 3 for three different isotherms. The dashed red line depicts the isotherm $T = 10$ MeV, at half the critical temperature. X_α increases smoothly with chemical potential until reaching the liquid-gas coexistence curve. Higher values of μ correspond to a dense liquid composed mainly of nucleons. The α mass fraction drops to negligibly small values in the liquid phase. As mentioned above, only the globally stable thermodynamic states are considered. The metastable parts of the $T = 10$ MeV isotherm (which also exist) are not shown in Fig. 3.

FIG. 2. Contour plots of the baryonic density n_B (a) and of the "mass fraction" of the α particles (b) in the (μ_B, T) plane. The solid lines depict the phase transition curve. The full circles correspond to the critical end point.
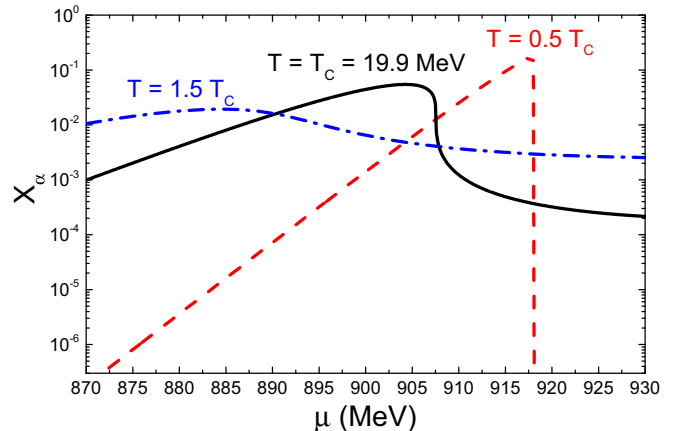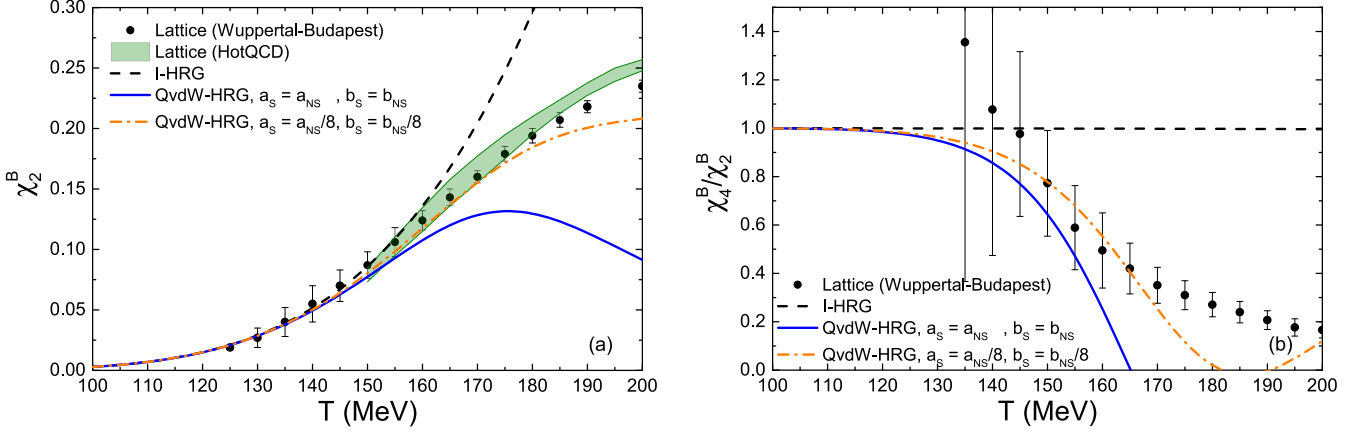
FIG. 4. The temperature dependence of (a) χ_2^B and (b) χ_4^B/χ_2^B net baryon number susceptibilities, as calculated within the I-HRG model (dashed black lines), the QvdW-HRG model with $a_S = a_{NS}$ and $\tilde{b}_S = \tilde{b}_{NS}$ (solid blue lines), and the QvdW-HRG model with $a_S = a_{NS}/8$ and $\tilde{b}_S = \tilde{b}_{NS}/8$ (dash-dotted orange lines) at zero chemical potential. The lattice QCD results of the Wuppertal-Budapest [30,31] and HotQCD [32] collaborations are shown, respectively, by symbols and green bands.

The behavior of X_α at the critical isotherm $T = T_c$ (solid black line in Fig. 3) is qualitatively similar to the previous one. X_α exhibits a rapid, but continuous drop at CP and in the vicinity of the CP along the critical isotherm. This correlates with a rapid increase of the baryon density with μ across the critical isotherm near the CP.

Finally, the isotherm $T = 3 T_c / 2 \simeq 30$ MeV in the crossover region is shown in Fig. 3 as the dash-dotted blue line. The μ dependence of X_α shows a broad maximum at this isotherm. This bump corresponds to the crossover region of the phase diagram (Fig. 2), where a smooth increase of the baryon density with μ takes place.

The example presented in this subsection shows that the repulsive vdW interactions cause the cluster dissolution at high baryonic densities. This conclusion is not new: The EV interactions had previously been used in relativistic mean-field models of nuclear matter [23–25]. More realistic studies of nuclear matter must also take into account the attractive interactions involving α particles.

Presented studies can be extended. For instance, only globally stable thermodynamic states of the N-α mixture were considered in this work: the Gibbs criterion in the GCE was applied. A more complete picture can be obtained by additionally analyzing metastable and unstable states. This work assumes that α particles do not form Bose-Einstein condensates. The effects of Bose-Einstein condensates of α particles could play a significant role [26], especially at low temperatures. Other nuclear clusters, such as d, t, etc., should be included in the description of nuclear matter as well [7].

C. Flavor-dependent vdW interactions in HRG and lattice data at $\mu_B = 0$

Flavor-dependent vdW interactions in the HRG model can be considered in the context of the lattice QCD data. The strong influence of the baryon-baryon vdW interactions was demonstrated for observables accessible with lattice QCD at zero chemical potential in the crossover region [17], using identical vdW interactions between only (anti)baryon

pairs. The vdW terms between all other hadron pairs were neglected in Ref. [17]. This simplest scenario can be modeled essentially with a single-component quantum statistical vdW model. Evidently, different baryon pairs may have different vdW parameters. Heavier strange hadrons may have different parameters compared to nonstrange ones, e.g., a smaller size. A thermal analysis of the hadron yield data [27] suggests this possibility.

Presently vdW interactions are included only for (anti)baryon pairs, similarly to Ref. [17]. We extend the QvdW-HRG model[1] of Ref. [17] by considering grossly different vdW parameters for nonstrange and strange baryons. The vdW parameters which reproduce properties of the nuclear ground state [15] are employed for all pairs of nonstrange baryons, i.e., $a_{NS} = 329$ MeV fm^3 and $\tilde{b}_{NS} = 3.42$ fm^3. The effective hard-core radius of strange baryons is assumed to be half that of nonstrange baryons. Hence, the EV parameter b_S of a strange baryon is 8 times smaller than the EV parameter b_{NS} of nonstrange baryon. The attractive vdW parameters a_{NS} here are assumed to be also a factor 8 smaller then the nonstrange ones. Thus, $a_S = a_{NS}/8 \simeq 41$ MeV fm^3 and $\tilde{b}_S = \tilde{b}_{NS}/8 \simeq 0.43$ fm^3.

A large, factor 8, difference between vdW parameters for strange and nonstrange baryons in the present toy model illustrates the multicomponent vdW formalism. Obviously, a different scenario with revised values of these parameters may be considered as well. The vdW interactions between strange and nonstrange baryons are characterized by the corresponding cross-term coefficients. The repulsive cross-term coefficients $\tilde{b}_{ij}$ are calculated according to Eq. (2). The attractive cross-term coefficients a_{ij} are calculated as a geometric mean, i.e.,

$$a_{ij} = \sqrt{a_i a_j}. \qquad (35)$$

This particular mixing rule is motivated by its common use in chemistry [28,29].

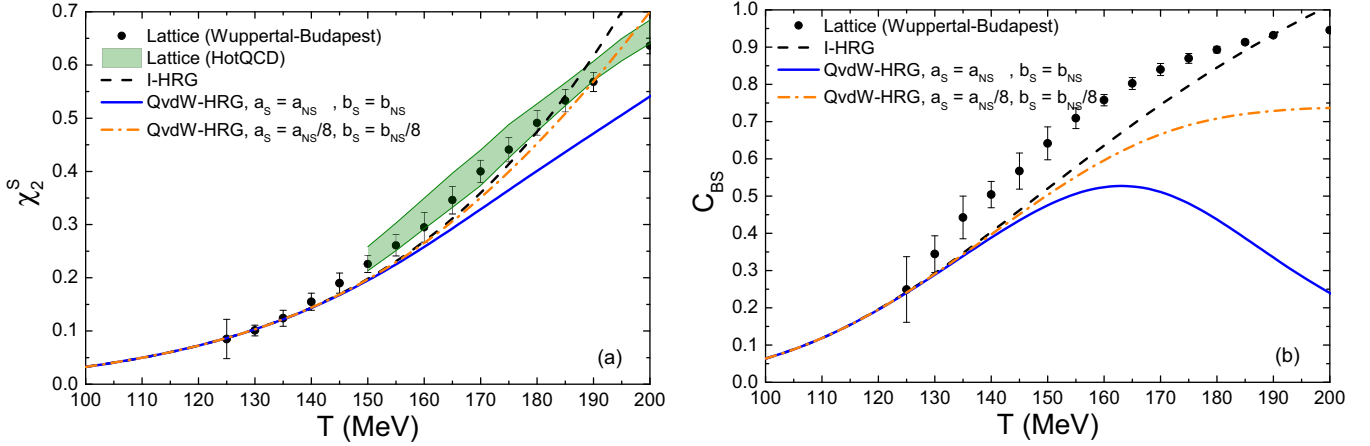[1]In the notation of Ref. [17] it is referred to as the VDW-HRG model.

FIG. 5. The temperature dependence of (a) net-strangeness susceptibility χ_2^S and (b) baryon-strangeness correlator ratio $C_{BS} = -3\,\chi_{11}^{BS}/\chi_2^S$, as calculated within the I-HRG model (dashed black lines), the QvdW-HRG model with $a_S = a_{NS}$ and $\tilde{b}_S = \tilde{b}_{NS}$ (solid blue lines), and the QvdW-HRG model with $a_S = a_{NS}/8$ and $\tilde{b}_S = \tilde{b}_{NS}/8$ (dash-dotted orange lines) at zero chemical potential. The lattice QCD results of the Wuppertal-Budapest [30] and HotQCD [32] collaborations are shown, respectively, by symbols and green bands.

The temperature dependencies of the net baryon susceptibilities χ_2^B and χ_4^B/χ_2^B at $\mu = 0$ are calculated for the different models: Within the I-HRG model, the QvdW-HRG model with $a_S = a_{NS}$ and $\tilde{b}_S = \tilde{b}_{NS}$, and the QvdW-HRG model with $a_S = a_{NS}/8$ and $\tilde{b}_S = \tilde{b}_{NS}/8$. These dependencies are compared in Fig. 4 to the lattice QCD data of the Wuppertal-Budapest [30,31] and HotQCD [32] collaborations. The scenario with weaker vdW interactions involving strange baryons improves the agreement with the lattice data. This is primarily caused by the overall decrease of the effects of the repulsive EV interactions.

The strangeness observables are sensitive to vdW interactions of strange baryons. The net strangeness susceptibility χ_2^S and the baryon-strangeness correlator ratio $C_{BS} = -3\,\chi_{11}^{BS}/\chi_2^S$ are used to demonstrate this. The latter observable, suggested in Ref. [33], is particularly sensitive and therefore is a useful diagnostic tool for QCD matter. The calculations for these two observables are shown in Fig. 5. They are compared with the corresponding lattice results of the Wuppertal-Budapest [30] and HotQCD [32] collaborations.

The standard QvdW-HRG model (identical vdW parameters for both, the nonstrange and strange baryons) does not improve the agreement with the lattice data as compared to the I-HRG model for these observables. In fact, the agreement becomes significantly worse at high temperatures. In the scenario with the smaller vdW interactions for strange baryons, on the other hand, the existing agreement of the I-HRG model with the lattice QCD data for χ_2^S is preserved, see Fig. 5(a).

None of the considered scenarios describes the lattice data for the C_{BS} [Fig. 5(b)]: The lattice data are underestimated by all three models. The two QvdW-HRG models do show a characteristic inflection point in the temperature dependence of C_{BS}. This point seems to be present in the lattice QCD data as well. Reducing the vdW interactions of strange baryons does result in an improved agreement with the lattice QCD data. Hitherto undiscovered strange hadrons may be the source of the underestimation of C_{BS} in HRG models. These states have been predicted by the quark model [34,35] and by the lattice

QCD spectrum calculations [36]. The agreement between the lattice QCD data and the I-HRG model for C_{BS} is improved if these extra states are included into the I-HRG model [37]. A similar effect is expected for all QvdW-HRG based models.

V. SUMMARY

This paper presented a generalization of the van der Waals equation of state for a multicomponent system. The formalism takes into account both the repulsive and the attractive interactions between particles of different species. It allows to specify the parameters characterizing repulsive and attractive forces between each pair of species independently. The quantum statistical effects, absent in the classical van der Waals equation, are introduced into the free energy of the multicomponent van der Waals model. The grand-canonical ensemble formulation of the model is also presented.

Both the grand-canonical formulation and the implementation of the quantum statistics in the multicomponent van der Waals model have been done in the present paper for the first time. These extensions are useful for many physical applications. The quantum statistical formulation is helpful for describing the asymmetric nuclear matter, which consists of an unequal number of interacting protons and neutrons. The formulation also allows treatment of the light nuclei in dense nuclear matter. The repulsive and attractive van der Waals interactions seem to be crucially important for baryons and antibaryons in hot hadronic matter. Such an application of the multicomponent van der Waals model is discussed in the present paper in the context of the strangeness dependent interactions. The formalism developed in this paper should be also useful for studies of the multicomponent systems of interacting atoms and molecules at small temperatures, where the quantum statistical effects are important.

[1] A. Mekjian, Phys. Rev. Lett. **38**, 640 (1977).

[2] J. Gosset, J. I. Kapusta, and G. D. Westfall, Phys. Rev. C **18**, 844 (1978).

[3] A. Z. Mekjian, Nucl. Phys. A **312**, 491 (1978).

[4] H. Stoecker, A. A. Ogloblin, and W. Greiner, Z. Phys. A **303**, 259 (1981).

[5] L. P. Csernai and J. I. Kapusta, Phys. Rept. **131**, 223 (1986).

[6] D. Hahn and H. Stocker, Phys. Rev. C **35**, 1311 (1987).

[7] D. Hahn and H. Stoecker, Nucl. Phys. A **476**, 718 (1988).

[8] J. Cleymans and H. Satz, Z. Phys. C **57**, 135 (1993).

[9] P. Braun-Munzinger and J. Stachel, Nucl. Phys. A **606**, 320 (1996).

[10] F. Becattini, J. Cleymans, A. Keranen, E. Suhonen, and K. Redlich, Phys. Rev. C **64**, 024901 (2001).

[11] P. Braun-Munzinger, V. Koch, T. Schäfer, and J. Stachel, Phys. Rept. **621**, 76 (2016).

[12] D. H. Rischke, M. I. Gorenstein, H. Stoecker, and W. Greiner, Z. Phys. C **51**, 485 (1991).

[13] L. M. Satarov, M. N. Dmitriev, and I. N. Mishustin, Phys. Atom. Nucl. **72**, 1390 (2009).

[14] L. M. Satarov, V. Vovchenko, P. Alba, M. I. Gorenstein, and H. Stoecker, Phys. Rev. C **95**, 024902 (2017).

[15] V. Vovchenko, D. V. Anchishkin, and M. I. Gorenstein, Phys. Rev. C **91**, 064314 (2015).

[16] D. Anchishkin and V. Vovchenko, J. Phys. G **42**, 105102 (2015).

[17] V. Vovchenko, M. I. Gorenstein, and H. Stoecker, Phys. Rev. Lett. **118**, 182301 (2017).

[18] V. Vovchenko, D. V. Anchishkin, and M. I. Gorenstein, J. Phys. A **48**, 305001 (2015).

[19] M. I. Gorenstein, A. P. Kostyuk, and Y. D. Krivenko, J. Phys. G **25**, L75 (1999).

[20] R. V. Poberezhnyuk, V. Vovchenko, D. V. Anchishkin, and M. I. Gorenstein, J. Phys. G **43**, 095105 (2016).

[21] K. Redlich and K. Zalewski, Acta Phys. Polon. B **47**, 1943 (2016).

[22] M. Dutra, O. Lourenço, S. S. Avancini, B. V. Carlson, A. Delfino, D. P. Menezes, C. Providência, S. Typel, and J. R. Stone, Phys. Rev. C **90**, 055203 (2014).

[23] J. M. Lattimer and F. D. Swesty, Nucl. Phys. A **535**, 331 (1991).

[24] S. Typel, Eur. Phys. J. A **52**, 16 (2016).

[25] H. Shen, H. Toki, K. Oyamatsu, and K. Sumiyoshi, Prog. Theor. Phys. **100**, 1013 (1998).

[26] L. Satarov, M. Gorenstein, A. Motornenko, V. Vovchenko, I. N. Mishustin, and H. Stoecker, J. Phys. G (2017), doi:10.1088/1361-6471/aa8c5d.

[27] P. Alba, V. Vovchenko, M. I. Gorenstein, and H. Stoecker, arXiv:1606.06542 [hep-ph].

[28] N. C. Patel and A. S. Teja, Chem. Eng. Sci. **37**, 463 (1982).

[29] J. V. Sengers, R. F. Kayser, C. J. Peters, and H. J. White, *Equations of State for Fluids and Fluid Mixtures* (Elsevier, Amsterdam, 2000).

[30] S. Borsanyi, Z. Fodor, S. D. Katz, S. Krieg, C. Ratti, and K. Szabo, J. High Energy Phys. 01 (2012) 138.

[31] R. Bellwied, S. Borsanyi, Z. Fodor, S. D. Katz, A. Pasztor, C. Ratti, and K. K. Szabo, Phys. Rev. D **92**, 114505 (2015).

[32] A. Bazavov, T. Bhattacharya, C. E. DeTar, H.-T. Ding, S. Gottlieb, R. Gupta, P. Hegde, U. M. Heller, F. Karsch, E. Laermann, L. Levkova, S. Mukherjee, P. Petreczky, C. Schmidt, R. A. Soltz, W. Soeldner, R. Sugar, and P. M. Vranas (HotQCD Collaboration), Phys. Rev. D **86**, 034509 (2012).

[33] V. Koch, A. Majumder, and J. Randrup, Phys. Rev. Lett. **95**, 182301 (2005).

[34] S. Capstick and N. Isgur, Phys. Rev. D **34**, 2809 (1986) [AIP Conf. Proc. **132**, 267 (1985)].

[35] D. Ebert, R. N. Faustov, and V. O. Galkin, Phys. Rev. D **79**, 114029 (2009).

[36] R. G. Edwards, N. Mathur, D. G. Richards, and S. J. Wallace (Hadron Spectrum Collaboration), Phys. Rev. D **87**, 054506 (2013).

[37] A. Bazavov, H. T. Ding, P. Hegde, O. Kaczmarek, F. Karsch, E. Laermann, Y. Maezawa, S. Mukherjee, H. Ohno, P. Petreczky, C. Schmidt, S. Sharma, W. Soeldner, and M. Wagner, Phys. Rev. Lett. **113**, 072001 (2014).